1. Maciej GWOZDZIEWICZ[1], 2. Marek CIURYS[1]

Wroclaw University of Science and Technology (1)
ORCID: 1. 0000-0002-8725-6679; 2. 0000-0002-7811-2198

Line Start Permanent Magnet Synchronous Motorrotor designing methodology

Abstract. In the paper methodology of Line Start Permanent Magnet Synchronous Motors rotor designing is proposed. The proposed methodology is based on four medium power low-voltage LSPMSM with numbers of pole pairs 2p=2, 4, 6 and 8. Both electrical properties and mechanical stresses are analysed. Electrical properties are based on magnetic field in air gap, back electromotive force and cogging torque. Mechanical stresses are considered due to centrifugal force and load torque. Proposed in the article colourful table with scores adequate to the obtained results of the investigated motor parameters can be convenient tool in machine designing.

Streszczenie. W artykule przedstawiono metodykę projektowania wirnika silników synchronicznych z magnesami trwałymi. Zaproponowana metodyka projektowania bazuje na silnikach typu LSPMSM średniej mocy niskiego napięcia o liczbie biegunów 2p=2, 4, 6 i 8. W trakcie badań brano pod uwagę zarówno właściwości elektromagnetyczne jak i również naprężenia mechaniczne. Właściwości elektromagnetyczne bazują na dystrybucji pola magnetycznego w szczelinie powietrznej, siły elektromotorycznej i momencie zaczepowym. Naprężenia mechaniczne bazują na siłach odśrodkowych oraz momencie obciążenia. Zaproponowano przedstawienie wyników badań w formie kolorowych tabel ułatwiających analizę otrzymanych wyników. (Metodyka projektowania wirnika silnika synchronicznego z magnesami trwałymi o rozruchu bezpośrednim)

Keywords: LSPMSM, permanent magnet, synchronous motor, mechanical stresses
Słowa kluczowe: LSPMSM, magnesy trwałe, silnik synchroniczny, naprężenia mechaniczne

Introduction

Electric motors are responsible for about 70% of electricity consumption in industry and for about 30-40% of electricity generated worldwide [1–3].

There are many design solutions for electric motors, however, three-phase squirrel-cage induction motors are the most commonly used [1–3], especially for a rated power of less than 10 kW [4]. This is due to their advantages such as: simplicity of construction, low production costs, high reliability (for example due to the lack of brushes and commutator) and relatively low operating costs.

The disadvantage of these motors is the low power factor [5], which additionally depends on the motor load. Low power factor is associated with an increase in reactive power. This results in an increase of supply currents, additional transmission losses and reduction in the possibility of loading generators and transformers with active power. In the case of too low power factor on the industrial facility side, reactive power compensation is required, which involves additional costs.

The development of high-energy permanent magnets, especially neodymium magnets, has resulted in progress in the construction of electrical machines. It led to the development of, among others, Permanent Magnet Synchronous Motors (PMSM), Brushless DC Motors (BLDCM), Brushless Synchronous Motors (BLSM), Permanent Magnet Direct Current Motors (PMDCM) as well as the development of Line Start Permanent Magnet Synchronous Motors (LSPMSM).

The efficiency of permanent magnet motors is higher than that of induction motors, especially for low power range [1, 2]. PM motors also have higher power factor and higher rated power density [4]. For these reasons, in the case of single-speed drives where the motor is powered directly from the mains, LSPMS motors are a good alternative to squirrel-cage induction motors [6].

In terms of the construction of the stator of LSPMSM, these motors are similar to induction motors. They have a three-phase winding placed in the slots of the magnetic circuit. In order to reduce eddy current power losses, magnetic circuit is made in the form of a package of electrotechnical sheets, usually 0.5 mm thick. In principle, a stator derived from typical squirrel-cage motors can be used to build LSPMS motors.

Inside the rotor of LSPMS machines there is a cage winding and permanent mag-nets, which are configured in U-type, V-type or W-type configuration in order to obtain the distribution of magnetic flux density in the air gap as close to sinusoidal as possible. The motor cage is used to start the machine [5, 7] and bring the motor speed near to synchronous one. It works only at the starting process [8], while the permanent magnets are used to pull rotor into synchronous speed [9] and to generate synchronous torque at steady state condition [5, 7]. Due to their parameters (high induction value, high energy density), neodymium magnets are most often used for this purpose.

The magnetic circuit of the rotor is most often made in the form of a package of electrotechnical sheets in order to limit eddy current power losses in it in dynamic states (e.g. during machine start-up). Due to the location of the magnets inside the rotor, they are better protected against demagnetization by high starting currents than in the case of motors with surface-mounted magnets [10, 11] such as BLDC motors, for example. However, when designing a motor with permanent magnets, one should also take into account the effect of temperature on the parameters of the magnets and their resistance to demagnetization [11].

Line start permanent magnet synchronous motors have many advantages [3, 6–10, 12–17]. In steady states LSPMS motors run at synchronous speed, therefore copper losses in the rotor cage are negligible [5, 7–9]. Their efficiency is very high [5, 6, 9, 10, 12, 13, 18], these motors are able to fulfil IE5 or even IE6 efficiency class requirements [19, 20]. They also have good thermal performances [6, 18]. The cost of LSPMSM is higher than induction motors of the same rated power, but the lower electricity costs due to the higher efficiency of these motors can quickly pay for themselves, which is an attractive solution from an economic point of view. The use of permanent magnets in the LSPMSM rotor ensures high value of the magnetic flux, which provides a high value of the power factor and high synchronizing torque. However, it results in a smaller cross-sectional area for the starting cage, thus the synchronization of the electric motor is more difficult [12]. The presence of permanent magnets in the

rotor is also associated with the fact that the magnets produce a braking torque [10, 12, 13] present during asynchronous operation of the machine. For this reasons, LSPMS motors have lower starting properties than induction motors [12].

Problems with the synchronization of LSPMS motors are also influenced, among others, by: high value of the load torque, high moment of inertia [16] of the drive system as well as the low power supply quality.

Due to problems with starting and synchronization, line started permanent mag-net synchronous motors are recommended for low starting demand torque applications like pumps, fans, textile machinery and compressors. According to [4] more than 50% of the motors that are used in industry are used in fan and pump drives. Therefore even a small difference in efficiency has a significant impact on energy savings.

Although many advantages of Line Start Permanent Magnet Synchronous Motors they are still not as popular as Induction Motors. This situation caused development of laser cutting of magnetic sheets for LSPMSMs what is optimal taking into account cost of machine production. The example of laser cutting of magnetic sheets is presented in Figure 1.

Fig.1. Laser cutting of Permanent magnet synchronous motor magnetic sheets. Photo courtesy of Kisielewski sp z.o.o.

Line Start Permanent Magnet Synchronous Motor model

Four fully parametrized line start permanent magnet synchronous motor FEM 2D models were built: Sm 315M2, Sm 315M4, Sm 315M6 and Sm 315M8. All models have the same outer stator diameter D_{out} = 470 mm. The 6-pole and 8-pole motor models have the same inner diameter D_{inner} = 330 mm and stator sheets what is not optimal for them but favourable taking into account motor standardization and production costs. Three-phase double layer, star connected stator winding was applied. Rotors squirrel cages consist of round brass bars. Rotors slots openings have width B_{r0} = 3.0 mm and height H_{r0} = 3.0 mm. Inside the rotor of LSPMS machines there are W-type configured permanent magnets. For all motors models each pole has four pieces of permanent magnets. The material of PMs is N40SH with the residual induction B_r = 1,27 T and coercivity H_c = 960 kA/m. All motors models are shown in Figure 2 and their parameters are presented in Table 1.

Table 1. Line Start Permanent Magnet Synchronous Motor models parameters

Motor	Sm315 M2	Sm315 M4	Sm315 M6	Sm315 M8
U_n [V]	400			
P_n [kW]	160	160	110	90
n_n [rpm]	3000	1500	1000	750
D_{outer} [mm]	470			
D_{inner} [mm]	270	310	330	330
Q_s [-]	48	60	72	72
L_{Fe} [mm]	360	390	350	390
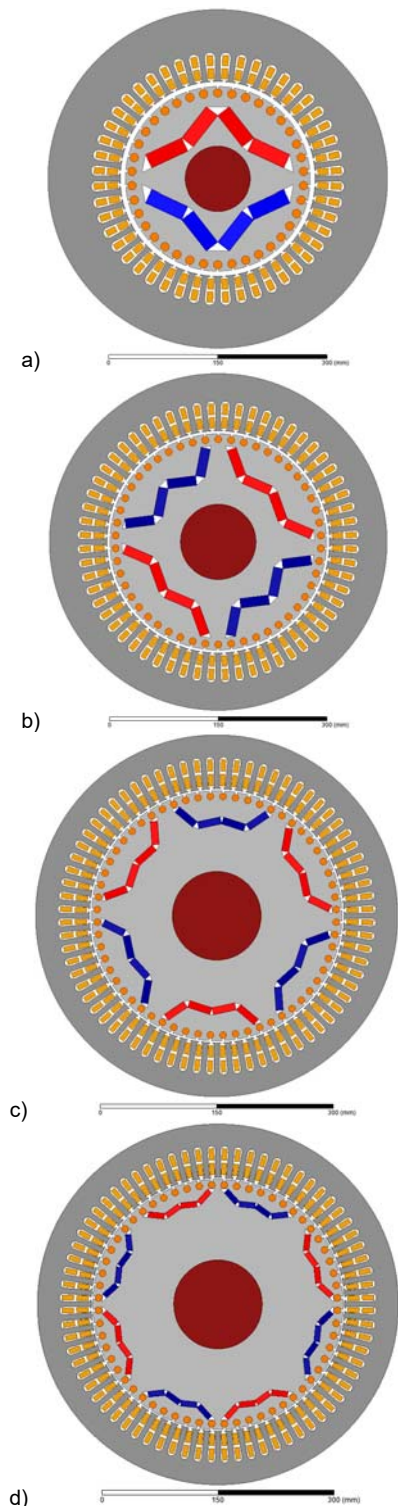
Fig.2. Line Start Permanent Magnet Synchronous Motor models: (a) Sm 315M2; (b) Sm 315M4; (c) Sm 315M6; (d) Sm 315M8

Mechanical computation

Line start permanent magnet synchronous motor rotor have openwork construction due many squirrel cage and permanent magnet slots. The biggest problem is extremely narrow distance between far permanent magnet slots of the magnetic pole and the nearest the pole squirrel cage slots H_{QrQm} which is illustrated in Figure 3. This dimension should be as low as possible to decrease permanent magnet leakage flux which is shown in Figure 4. Taking into account mechanical stresses due to rotational speed and load torque this dimension should be as high as possible. These two requirements are excluding each other.
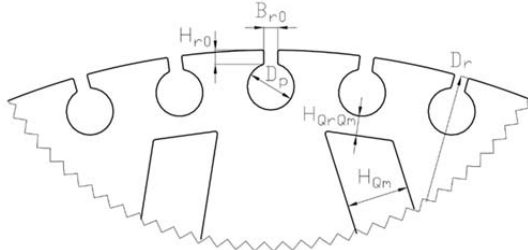
Fig.3. Line Start Permanent Magnet Synchronous Motor rotor construction in Sm 315M4
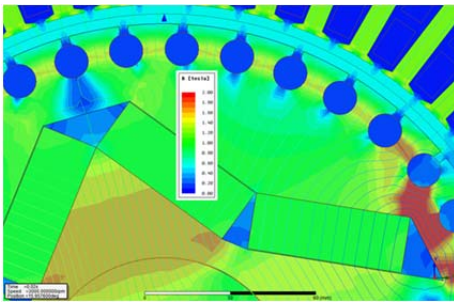
Fig.4. Permanent magnet leakage flux in Sm 315M2

During mechanical stresses analyses in Sm 315M2, Sm 315M4, Sm 315M6 and Sm 315M8 the following loads were taken into account:
— rotational speed $n = 1.2n_n$ and load torque $t_{load} = 0$,
— rotational speed $n = 1.0n_n$ and load torque $t_{load} = 10t_n$,
— gravity force perpendicular to the rotor sheet caught by its edges.

Due to the maximum mechanical stresses between squirrel cage slots and far permanent magnet slots the motor models meshes in this region were denser (Figure 5). configuration
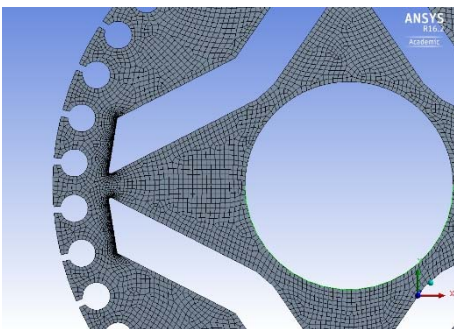
Fig.5. Sm 315M2 motor model for mechanical stresses analyses

Mechanical stresses in machines can be decreased not only by increasing machine parts dimensions but also by rounding corners of these parts. In case of laser cutting motor sheets the minimum radius of corners is 0.3 mm and optimum value is 0.5 mm. Influence of the permanent magnet slots corners radius in Sm 315M2 motor for

rotational speed $n = 1.2n_n$ without load torque is presented in Figure 6. The obtained results shows significant influence of the corners radius on mechanical stresses due to centrifugal force. Therefore for further investigation permanent magnet slots corner radius for all motors was assumed $R_{PM\_corner} = 1.0$ mm.

In Figures 7-10 results of mechanical stresses due to centrifugal force load torque and gravity for all motors are presented. Rotors sheets of the motors have the distance between far permanent magnet slots of the magnetic pole and the nearest the pole squirrel cage slot H_{QrQm} (Figure 3). On the basis of a series of computations, this dimension should be selected so as to obtain the mechanical stress at the maximum assumed level. In the work, this value was assumed as not greater than half of the rotor sheet yield strength. For 2-pole LSPMSM the maximum mechanical stresses occurs for rotational speed $n = 1.2n_n$ so for 2-pole LSPMSM centrifugal force determines the distance H_{QrQm}. For higher number of the motor pole pairs than 2 the distance H_{QrQm} is lower and mechanical stresses due to gravity is more significant. For Sm 315M8 the maximum mechanical stresses is caused by gravity which determines the distance H_{QrQm}.

a)

b)

c)
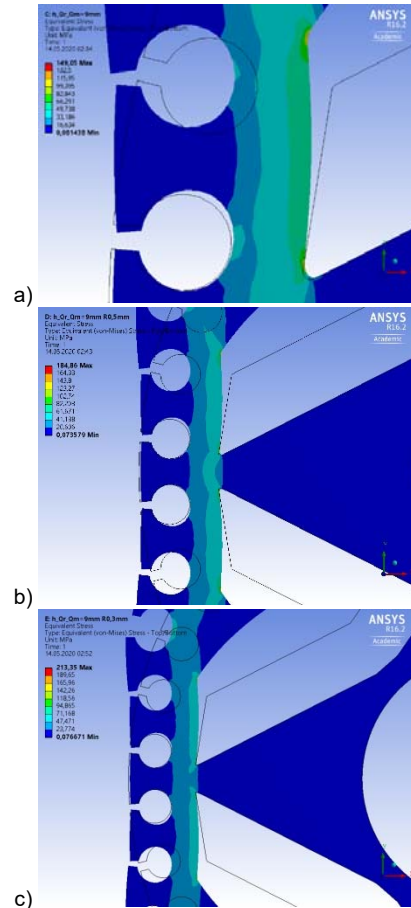
Fig.6. Sm 315M2 motor model for mechanical stresses analyses

a)

b)

c)
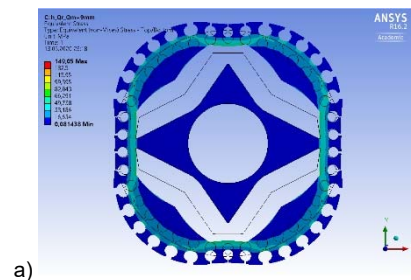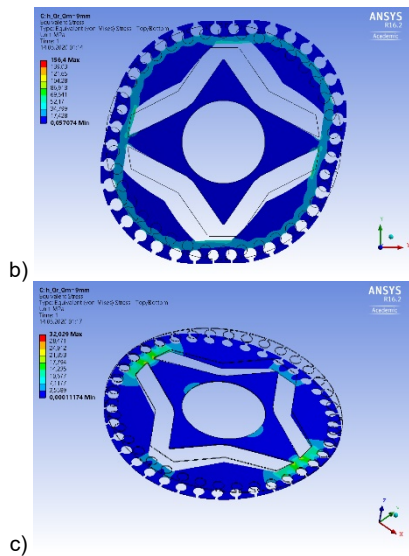
Fig.7. Mechanical stresses for Sm 315M2 rotor sheet motor for: (a) $n = 1.2n_n$ and $t_{load} = 0$; (b) $n = 1.0n_n$ and $t_{load} = 10t_n$; (c) gravity force perpendicular to the rotor sheet caught by its edges analyses

a)

b)

c)
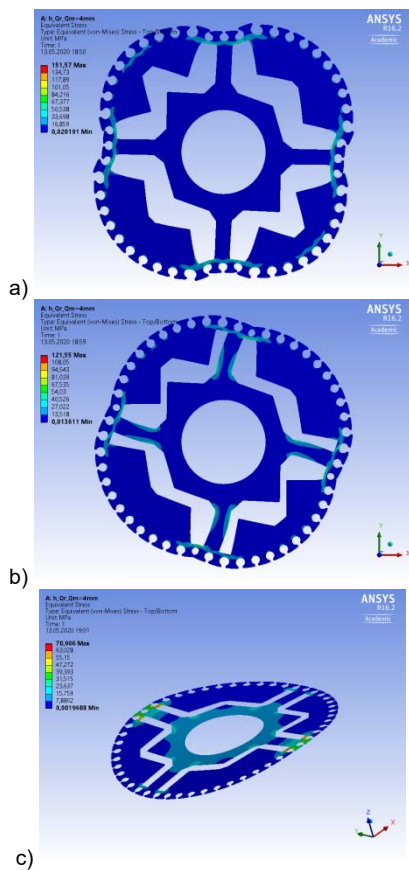
Fig.8. Mechanical stresses for Sm 315M4 rotor sheet motor for: (a) $n = 1.2n_n$ and $t_{load} = 0$; (b) $n = 1.0n_n$ and $t_{load} = 10t_n$; (c) gravity force perpendicular to the rotor sheet caught by its edges

a)

b)

c)
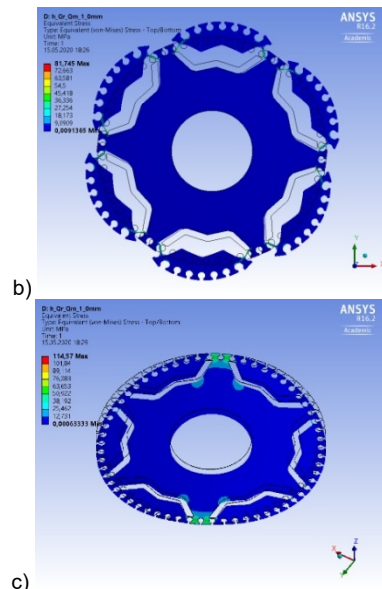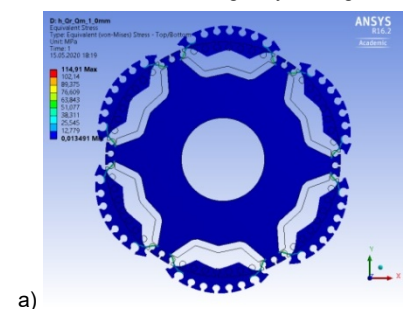
Fig.9. Mechanical stresses for Sm 315M6 rotor sheet motor for: (a) $n = 1.2n_n$ and $t_{load} = 0$; (b) $n = 1.0n_n$ and $t_{load} = 10t_n$; (c) gravity force perpendicular to the rotor sheet caught by its edges

a)

b)

c)
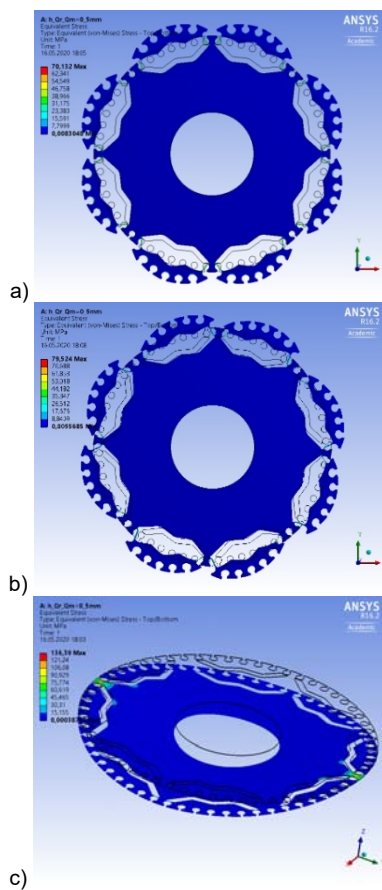
Fig.10. Mechanical stresses for Sm 315M8 rotor sheet motor for: (a) $n = 1.2n_n$ and $t_{load} = 0$; (b) $n = 1.0n_n$ and $t_{load} = 10t_n$; (c) gravity force perpendicular to the rotor sheet caught by its edges

Mechanical computation

The next step in permanent magnet synchronous motor designing is selection of the number of rotor slots. This number and permanent magnets arrangement deter-mines the magnetic field distribution which influences on back electromotive force *back EMF* and cogging torque. Back electromotive force was analysed by total harmonic distortion coefficient THD_E and cogging torque was investigated by peak-to-peak value T_{pk2pk}. For better

cogging torque computation accuracy motor models mesh in air gap was denser (Figure 11).
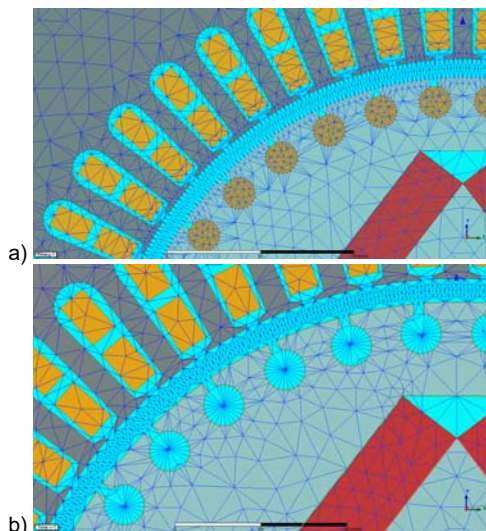
Fig.11. Sm 315M2 motor model mesh: (a) standard; (b) for cogging torque analysis
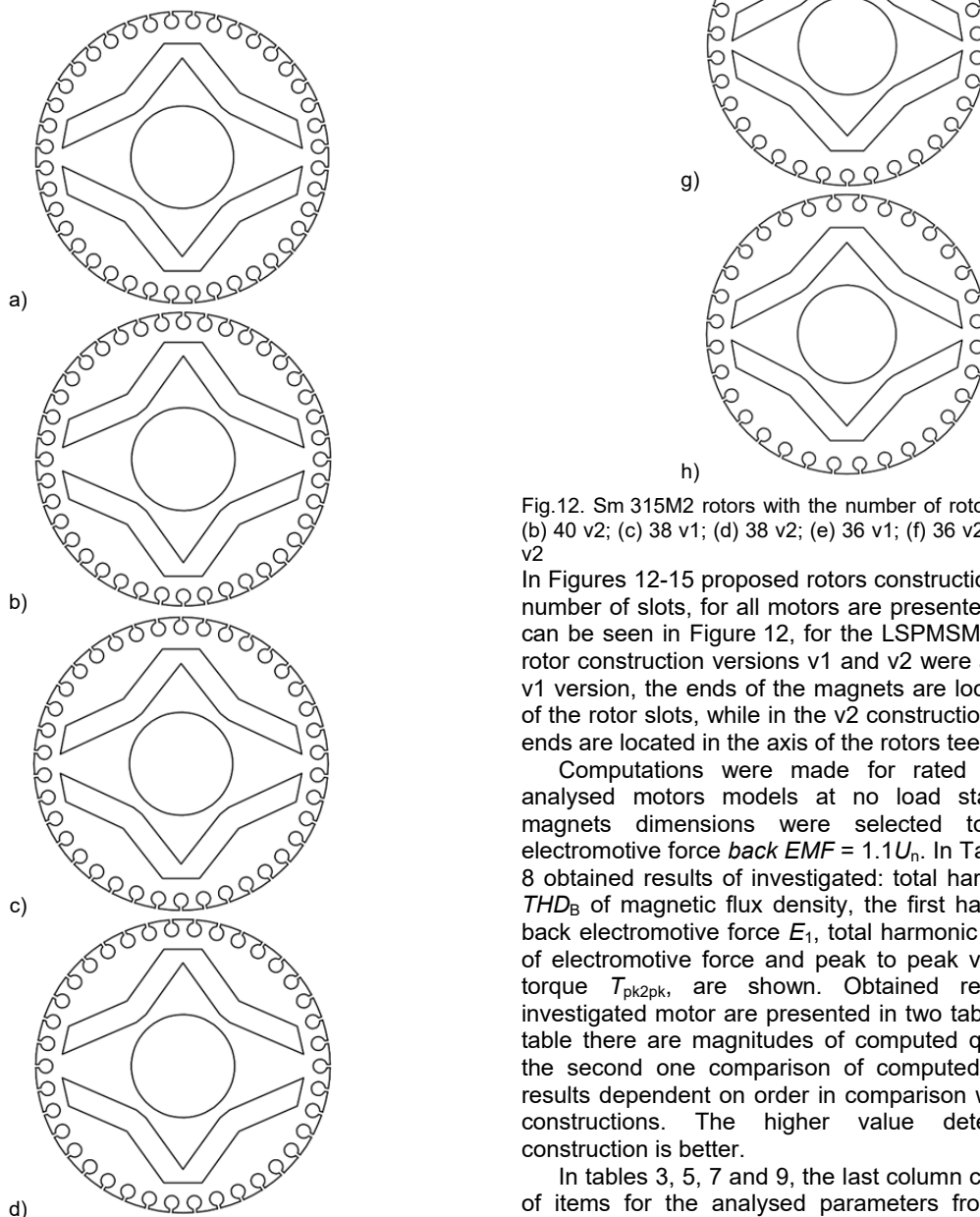
Fig.12. Sm 315M2 rotors with the number of rotor slots: (a) 40 v1; (b) 40 v2; (c) 38 v1; (d) 38 v2; (e) 36 v1; (f) 36 v2; (g) 34 v1; (h) 32 v2

In Figures 12-15 proposed rotors construction, with different number of slots, for all motors are presented. Moreover, as can be seen in Figure 12, for the LSPMSM Sm 315M2 two rotor construction versions v1 and v2 were analysed. In the v1 version, the ends of the magnets are located in the axis of the rotor slots, while in the v2 construction version, these ends are located in the axis of the rotors teeth.

Computations were made for rated speeds of the analysed motors models at no load state. Permanent magnets dimensions were selected to obtain back electromotive force *back EMF* = $1.1U_n$. In Tables 2, 4, 6 and 8 obtained results of investigated: total harmonic distortion THD_B of magnetic flux density, the first harmonic value of back electromotive force E_1, total harmonic distortion THD_E of electromotive force and peak to peak value of cogging torque T_{pk2pk}, are shown. Obtained results of every investigated motor are presented in two tables – in the first table there are magnitudes of computed quantities and in the second one comparison of computed quantities with results dependent on order in comparison with other motor constructions. The higher value determines which construction is better.

In tables 3, 5, 7 and 9, the last column contains the sum of items for the analysed parameters from the previous

columns. The higher total score determines which design solution is better. For easier comparison of obtained results they are coloured – for the best solution dark green and for the worst one red.

Table 2. Influence of the rotor slots number on the LSPMSM Sm 315M2 – obtained results

Q_r [-]	THD_B [%]	E_1 [V]	THD_E [%]	T_{pk2pk} [Nm]
40 v1	24.11	249.8	0.80	0.54
40 v2	23.52	249.0	0.60	0.23
38 v1	24.01	249.9	0.64	1.24
38 v2	24.03	248.1	0.67	1.60
36 v1	24.04	249.0	0.59	1.66
36 v2	23.49	247.8	0.61	2.53
34 v1	27.35	246.2	0.66	1.97
32 v1	26.91	246.2	0.65	3.28

Table 3. Influence of the rotor slots number on the LSPMSM Sm 315M2 – comparison

Q_r	THD_B	E_1	THD_E	T_{pk2pk}	Σ
40 v1	3	7	1	7	18
40 v2	7	6	7	8	28
38 v1	6	8	5	6	25
38 v2	5	4	2	5	16
36 v1	4	5	8	4	21
36 v2	8	3	6	2	19
34 v1	1	1	3	3	8
32 v1	2	2	4	1	9

The computational analysis carried out for the LSPMSM Sm 315M2 motor model showed that the best rotor construction is version v2 with 40 slots. For this design, the total number of points is 28 (Table 3). For this version of the rotor, the lowest value of the cogging torque, a high value of the first harmonic of back electromotive force E_1 and low values of total harmonic distortion THD_E and THD_B were obtained in comparison with other constructions (Table 2). The worst solutions are versions 32 v1 and 34 v1. For the solution with 34 slots of the rotor, the lowest value of E_1 and the highest THD_B were obtained.

For the LSPMSM with two pairs of poles, the versions with 46 and 50 rotor slots turned out to be the best solutions. They received 18 points each according to Table 5.

a)

b)

c)

d)

e)

f)
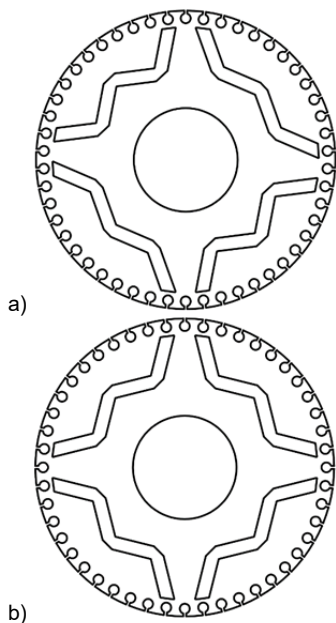
Fig.13. Sm 315M4 rotors with the number of rotor slots: (a) 50; (b) 48; (c) 46; (d) 44; (e) 42; (f) 40

Table 4. Influence of the rotor slots number on the LSPMSM Sm 315M4 – obtained results

Q_r [-]	THD_B [%]	E_1 [V]	THD_E [%]	T_{pk2pk} [Nm]
50	22.77	251.5	0.74	8.85
48	22.55	250.4	1.00	9.38
46	22.75	250.1	0.79	2.37
44	22.40	249.6	1.10	10.6
42	23.48	247.9	0.92	4.41
40	22.69	248.0	1.22	32.80

Table 5. Influence of the rotor slots number on the LSPMSM Sm 315M4 – comparison

Q_r	THD_B	E_1	THD_E	T_{pk2pk}	Σ
50	2	6	6	4	18
48	5	5	3	3	16
46	3	4	5	6	18
44	6	3	2	2	13
42	1	1	4	5	11
40	4	2	1	1	8

For the motor with 50 slots, the best result was obtained in terms of value of the first harmonic of back electromotive force E_1 and total harmonic distortion THD_E among all the analysed rotors constructions (Table 4). The 46-slots version has the lowest cogging torque and low THD_E. The

worst rotor construction is the one with 40 slots. For this design the highest value of the cogging torque and THD_E were obtained.

a)

b)

c)

d)

e)
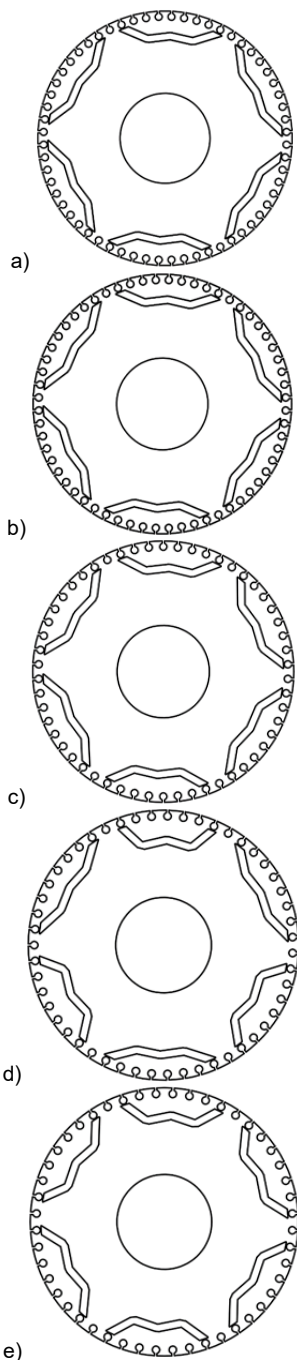
Fig.14. Sm 315M6 rotors with the number of rotor slots: (a) 60; (b) 57; (c) 54; (d) 51; (e) 48

The results of computations made for a different number of rotor slots in the 6-pole model showed that the best construction among the analysed designs is the one with 57 slots (Table 6). The 48-slot model is the worst. For the 57-slot model, the highest value of the first harmonic of back electromotive force E_1, the lowest THD_E, low THD_B and cogging torque were obtained. For the structure with 48 slots, the values of all analysed parameters were the worst (Table 6).

The computational analysis carried out for the LSPMSM Sm 315M8 motor model showed that the best rotor construction is version with 60 slots and the worst is the one with 48 slots (Tables 8 and 9). For the best design, the total

number of points is 14, while for the worst is only 5 (Table 9). For the 60 rotor slots construction version, the lowest value of the cogging torque and THD_E, a high value of the first harmonic of back electromotive force E_1 and a low value of total harmonic distortion THD_B, were obtained in comparison with other constructions (Table 8). For the structure with 48 slots, the values of almost all analysed parameters were the worst (Table 8).

Table 6. Influence of the rotor slots number on the LSPMSM Sm 315M6 – obtained results

Q_r [-]	THD_B [%]	E_1 [V]	THD_E [%]	T_{pk2pk} [Nm]
60	22.70	251.67	0.95	37.20
57	23.78	252.40	0.68	11.60
54	24.31	250.11	1.17	34.90
51	25.20	250.24	0.84	9.92
48	27.38	248.74	3.72	89.20

Table 7. Influence of the rotor slots number on the LSPMSM Sm 315M6 – comparison

Q_r	THD_B	E_1	THD_E	T_{pk2pk}	Σ
60	5	4	3	2	14
57	4	5	5	4	18
54	3	2	2	3	10
51	2	3	4	5	14
48	1	1	1	1	4

a)

b)

c)

d)
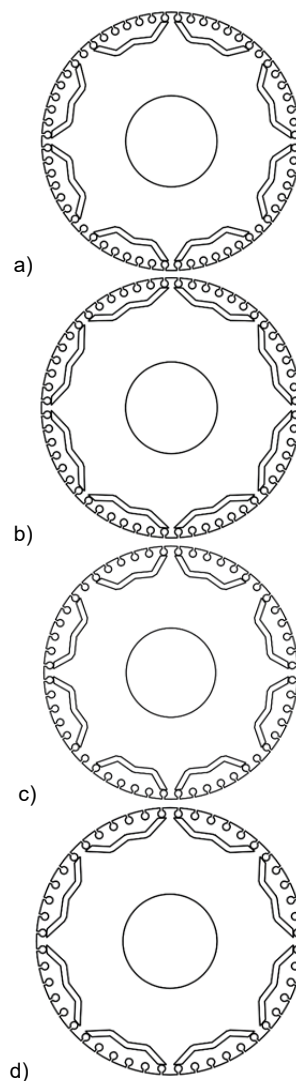
Fig.15. Sm 315M8 rotors with the number of rotor slots: (a) 60; (b) 56; (c) 52; (d) 48

Table 8. Influence of the rotor slots number on the LSPMSM Sm 315M8 – obtained results

Q_r [-]	THD_B [%]	E_1 [V]	THD_E [%]	T_{pk2pk} [Nm]
60	29.73	253.1	0.92	6.93
56	29.39	251.1	1.01	61.8
52	32.53	253.2	1.24	39.3
48	32.32	250.3	1.68	187

Table 9. Influence of the rotor slots number on the LSPMSM Sm 315M8 – comparison

Q_r	THD_B	E_1	THD_E	T_{pk2pk}	Σ
60	3	3	4	4	14
56	4	2	3	2	11
52	1	4	2	3	10
48	2	1	1	1	5

Conclusions

Line start permanent magnet synchronous motor rotor is an openwork construction which needs special computation to avoid too much mechanical stresses and too much permanent magnet leakage flux. For 2-pole medium power LSPMSM the most significant mechanical stress is caused by centrifugal force and for higher number of the pole pairs *2p* mechanical stress due to gravity force increases. For 8-pole medium power LSPMSM the distance between far permanent magnet slots of the magnetic pole and the nearest the pole squirrel cage slot H_{QrQm} is determined exactly by the gravity.

Proposed methodology of line start permanent magnet synchronous motor designing using colourful table with scores adequate to the obtained results of the investigated motor parameters can be convenient tool in machine designing. This applies especially to the number of LSPMSM rotor slots Q_r assortment taking into account such parameters like back electromotive force *back EMF* and its total harmonic distortion coefficient THD_E, magnetic induction in the air gap B_1 and its total harmonic distortion coefficient of THD_B and cogging torque T_{pk2pk}.

Authors: PhD Maciej Gwozdziewicz, Electrical Engineering Faculty at Wroclaw University of Science and Technology, wybrzeze Stanislawa Wyspianskiego 27, 50-370 Wroclaw, E-mail: *maciej.gwozdziewiczi@pwr.edu.pl*; Prof. Marek Ciurys, Electrical Engineering Faculty at Wroclaw University of Science and Technology, wybrzeze Stanislawa Wyspianskiego 27, 50-370 Wroclaw, E-mail: *marek.ciurys@pwr.edu.pl*

REFERENCES
[1] De Almeida, A.T.; Ferreira, F.J.T.E.; Fong, J.A.C. Standards for Efficiency of Electric Motors. *IEEE Ind. Appl. Mag.* **2011**, *17*, 12–19, doi:10.1109/MIAS.2010.939427.
[2] De Almeida, A.T.; Ferreira, F.J.T.E.; Baoming, G. Beyond Induction Motors—Technology Trends to Move Up Efficiency. *IEEE Trans. Ind. Appl.* **2014**, *50*, 2103–2114, doi:10.1109/TIA.2013.2288425.
[3] De Almeida, A. T.; Ferreira, F.J.T.E.; Duarte, A. Q. Technical and Economical Considerations on Super High-Efficiency Three-Phase Motors. *IEEE Transactions on Industry Applications* **2014**, vol. 50, no. 2, 1274-1285, doi: 10.1109/TIA.2013.2272548.
[4] Gieras, J.F. *Permanent Magnet Motor Technology: Design and Applications, Third Edition*; 3rd edition.; CRC Press: Boca Raton, 2009; ISBN 978-1-4200-6440-7.
[5] Fei, W.; Luk, P.C.K.; Ma, J.; Shen, J.X.; Yang, G. A High-Performance Line-Start Permanent Magnet Synchronous Motor Amended From a Small Industrial Three-Phase Induction Motor. *IEEE Transactions on Magnetics* **2009**, vol. 45, no. 10, 4724-4727, doi: 10.1109/TMAG.2009.2022179.
[6] Aliabad, A. D.; Ghoroghchian, F. Design and Analysis of a Two-Speed Line Start Synchronous Motor: Scheme One. *IEEE Transactions on Energy Conversion* **2016**, vol. 31, no. 1, 366-372, doi: 10.1109/TEC.2015.2481929.
[7] Knight, A.M.; McClay, C.I. The design of high-efficiency line-start motors. *IEEE Transactions on Industry Applications* **2000**, vol 36, issue 6, 1555 – 1562, doi: 10.1109/28.887206.
[8] Li, L.; Fu, W.; Niu, S. Novel Steel-Bar Starting Cage Line-Start Permanent Magnet Machine With Spoke-Type Insulation Layers. *IEEE Transactions on Magnetics* **2022**, vol. 58, no. 8, 1-5, doi: 10.1109/TMAG.2022.3154973.
[9] Dinh, B. M.; Tien, H. M. Maximum efficiency design of line start permanent magnet synchronous motor. 2016 IEEE International Conference on Sustainable Energy Technologies (ICSET), Hanoi, 2016, 350-354, doi: 10.1109/ICSET.2016.7811808.
[10] Ugale, R. T.; Chaudhari, B. N. Rotor Configurations for Improved Starting and Synchronous Performance of Line Start Permanent-Magnet Synchronous Motor. *IEEE Transactions on Industrial Electronics* **2017**, vol. 64, no. 1, 138-148, doi: 10.1109/TIE.2016.2606587.
[11] Zawilak T.; Gwozdziewicz, M. Demagnetization Process in Line Start Permanent Magnet Synchronous Motor. 2018 International Symposium on Electrical Machines (SME), 2018, 1-5, doi: 10.1109/ISEM.2018.8442933.
[12] Zawilak, T.; Antal, L. Porównanie silnika indukcyjnego z silnikiem synchronicznym z magnesami trwałymi i rozruchem bezpośrednim. *Prace Naukowe Instytutu Maszyn, Napędów i Pomiarów Elektrycznych Politechniki Wrocławskiej* **2005,** 58, Studia i Materiały, no. 25, 212-221, https://www.researchgate.net/publication/242761348_POROW NANIE_SILNIKA_INDUKCYJNEGO_Z_SILNIKIEM_SYNCHR ONICZNYM_Z_MAGNESAMI_TRWALYMI_I_ROZRUCHEM_B EZPOSREDNIM.
[13] Tian, M.; Wang, X.; Wang, D.; Zhao, W.; Li, C. A Novel Line-Start Permanent Magnet Synchronous Motor With 6/8 Pole Changing Stator Winding. *IEEE Transactions on Energy Conversion* **2018**, vol. 33, no. 3, 1164-1174, doi: 10.1109/TEC.2018.2826550.
[14] Knypiński, Ł.; Pawełoszek, K.; Le Menach, Y. Optimization of Low-Power Line-Start PM Motor Using Gray Wolf Metaheuristic Algorithm. *Energies* **2020**, 13, 1186. https://doi.org/10.3390/en13051186.
[15] Zhou, Y.; Huang, K.; Sun, P.; Dong, R. Analytical Calculation of Performance of Line-Start Permanent-Magnet Synchronous Motors Based on Multidamping-Circuit Model. *IEEE Transactions on Power Electronics* **2021**, vol. 36, no. 4, 4410-4419, doi: 10.1109/TPEL.2020.3025172.
[16] Jedryczka, C.; Wojciechowski, R. M.; Demenko, A. The influence of squirrel cage geometry on synchronization of line start permanent magnet synchronous motor. 9th IET International Conference on Computation in Electromagnetics (CEM 2014), 2014, 1-2, doi: 10.1049/cp.2014.0235.
[17] Hassanpour Isfahani, A.; Vaez-Zadeh, S. Effects of Magnetizing Inductance on Start-Up and Synchronization of Line-Start Permanent-Magnet Synchronous Motors. *IEEE Transactions on Magnetics* **2011**, 47, no. 4, 823-829, doi: 10.1109/TMAG.2010.2091651.
[18] Bao, Y.; Mehmood, W.; Feng, X. Super premium efficiency Line Start Permanent Magnet Synchronous Motor: Design, test and comparison. 2012 Petroleum and Chemical Industry Conference (PCIC), 2012, 1-7, doi: 10.1109/PCICON.2012.6549645.
[19] Gwozdziewicz, M.; Zawilak, J. Induced pole permanent magnet synchronous motor. 2017 International Symposium on Electrical Machines (SME), Naleczow, 2017, 1-4, doi: 10.1109/ISEM.2017.7993543.
[20] Gwozdziewicz, M.; Jankowska, K. Analysis of a new concept of Line Start Permanent Magnet Synchronous Motor. *Przeglad Elektrotechniczny* **2022***,* R.98, no. 8/2022, 168-173, doi:10.15199/48.2022.08.31.
[21] Gwozdziewicz, M.; Zawilak, J. Limitation of torque ripple in medium power line start permanent magnet synchronous motor. *Przeglad Elektrotechniczny* **2017***,* R.93, no.6/2017, 1-4, doi: 10.15199/48.2017.06.01.